DEVELOPMENT OF THE PACOSS D-STRUT™

David C. Cunningham[1]
Honeywell Inc., Satellite Systems Operation

ABSTRACT

This paper presents the design optimization procedure that was used to size the D-Struts™ used on the Passive/Active Control of Space Structures (PACOSS) program. While this design uses a diaphragm for the pumping member of the damper, the method can be adapted for other approaches. Fourteen D-Struts are fabricated and extensively characterized using the method of complex mechanical impedance. Performance agrees well with predictions, except that the peak phase lead is low. Additional compliance, which is responsibile for this loss in performance, is primarily due to the diaphragm flexing at its inner and outer edges. This paper suggests solutions to improve the diaphragm clamping as well as alternatives to using a diaphragm.

[1]Senior Staff Engineer, Honeywell Inc., Satellite Systems Operation,
P.O. Box 52199, Phoenix, AZ 85072, (602) 561-3211

INTRODUCTION

The viscously damped strut, or D-Strut™, was invented by L. Porter Davis and Dr. James F. Wilson to provide damping augmentation in a truss-type structure. The D-Strut consists of two concentric tubes, rigidly fastened together at one end, and connected through a viscous damper at the other. D-Struts can be used selectively in a truss-type structure to provide high damping of specific modes by placing them at locations of high modal strain energy. See the paper "Design, Analysis, and Testing of the PACOSS D-Strut Truss" by D. Morgenthaler in these proceedings for a discussion of this methodology.

THREE PARAMETER MODEL

The simplest dynamic model of the element is shown in Figure 1 and consists of three parameters: a stiffness representing the outer tube, a second stiffness representing the inner tube, and a viscous damper in series with the inner tube stiffness.

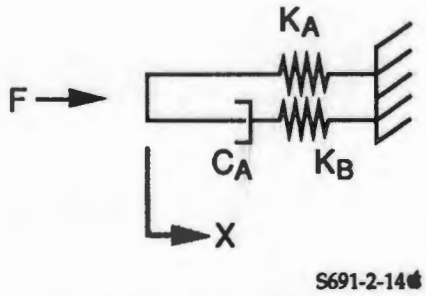

Figure 1. D-Strut Simplified Model

The ratio of force to deflection at one end, with the opposite end fixed, is the mechanical impedance, and it is given by:

$$Z3(s) = KA(1+s/w1)/(1+s/w2) \quad (1)$$

where,

$$\omega_1 = K_A K_B/(K_A+K_B)C_A \quad (2)$$

$$\omega_2 = K_B/C_A \quad (3)$$

The magnitude of Z3 is plotted against radian frequency in Figure 2. At frequencies below ω_1, the D-Strut acts like a "soft" spring, while at frequencies above ω_2, the D-Strut acts like a "stiff" spring. The phase shift follows a bell-shaped curve between ω_1 and ω_2. The maximum phase lead occurs at the geometric mean frequency:

$$\omega_0 = (\omega_1 \omega_2)^{1/2} \quad (4)$$

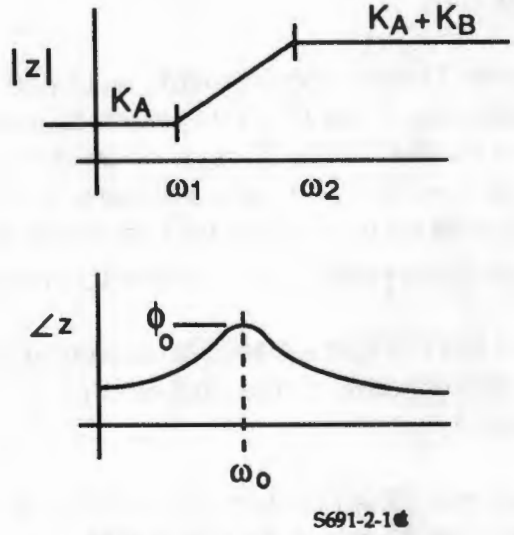

Figure 2. Mechanical Impedance

Letting α^2 denote the lead/lag separation ratio,

$$\alpha = (\omega_2/\omega_1)^{1/2} \tag{5}$$

the complex impedance at ω_0 is:

$$Z_3(j\omega_0) = K_A[2+j(\alpha-\alpha^{-1})]/(1+\alpha^{-2}) \tag{6}$$

The maximum phase lead is:

$$\phi(\omega_0) = \tan^{-1}[(\alpha-\alpha^{-1})/2] \tag{7}$$

When the D-Strut is used in a structure, damping will be proportional to the phase lead at any frequency. Maximum damping then occurs when the frequency of maximum phase lead is made to coincide with the resonant frequency to be damped. For example, if the D-Strut supports a simple mass, M, the damping ratio will be equal to:

$$\zeta = (\alpha-1)/2 \tag{8}$$

provided that the D-Strut is optimally tuned to the resonant frequency. This is accomplished by selecting the damping constant, C_A, such that:

$$\omega_0 = (\alpha K_A/M)^{1/2} \tag{9}$$

PACOSS REQUIREMENTS

For the PACOSS program, D-Strut requirements were defined by the contractor, Martin Marietta, to provide damping of the first two structural frequencies when D-Struts were used as the longerons in the lower 3 bays of an 8-bay truss structure. Figure 3 summarizes these requirements. The static stiffness is 78,000 lb/in., and the dynamic stiffness ($K_A + K_B$) is 179,000 lb/in. Maximum phase lead is 22.6 degrees and occurs at a frequency of 5.6 Hz; this corresponds to a 1.5 separation ratio, α.

The structural design of the D-Strut is based on accommodating a step function of force equal to 566 lb. (This corresponds to the longeron force developed by a 100-lb lateral load at the tip of the truss.)

Finally, the D-Strut is to meet the interface and outline dimensions shown in Figure 3. The maximum diameter indicated is to be minimized.

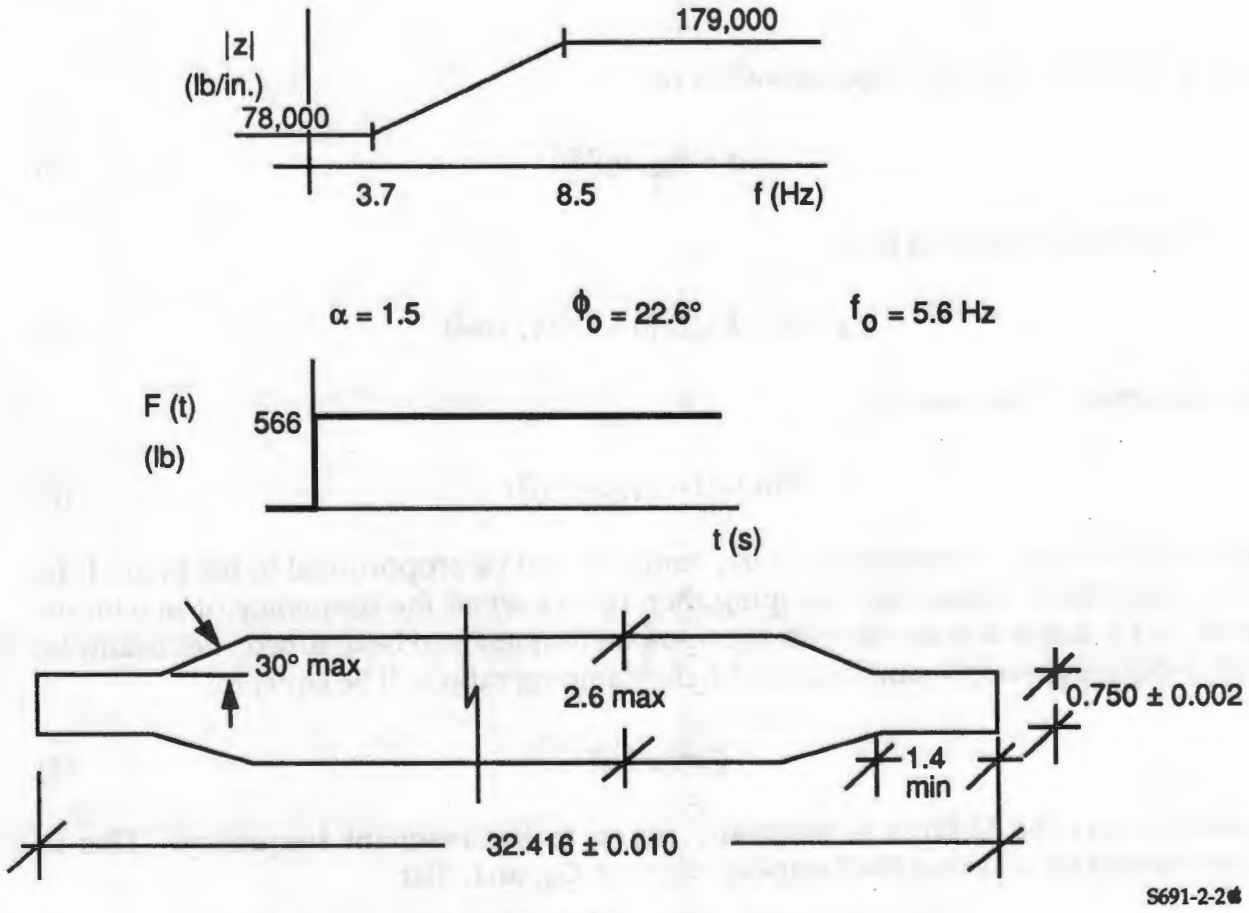

Figure 3. PACOSS D-Strut Design Requirements

DESIGN CONFIGURATION

Figure 4 is a conceptual view of the D-Strut showing the selected dimensions that provide the required performance. In this implementation, the viscous damper consists of a circular diaphragm connecting the inner and outer tubes. Viscous fluid is sheared in the orifice of length, L, and diameter, d, when the fluid is pumped by relative motion of the inner and outer tubes. The spring shown on the left provides a preload in the fluid contained by the bellows such that damping will occur in both forward and reverse directions.

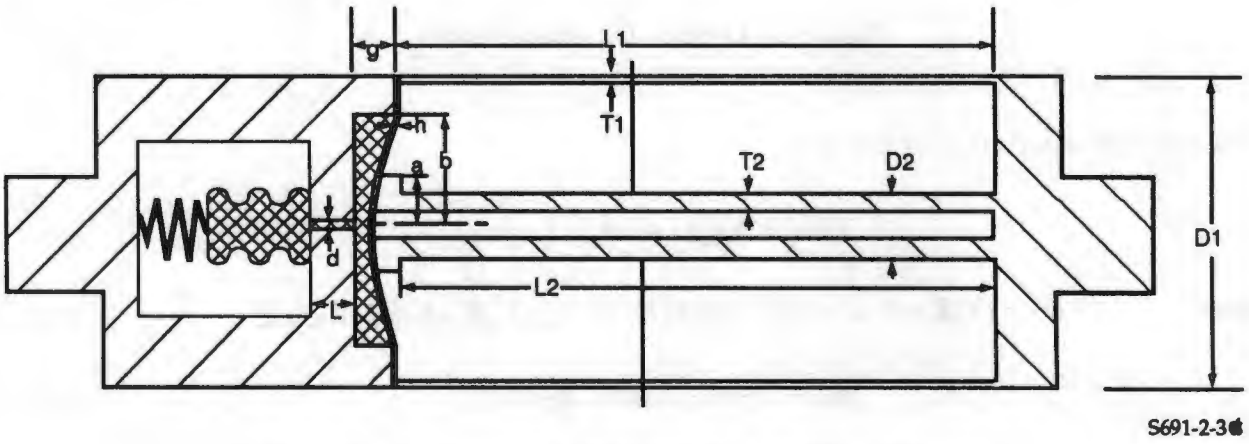

Figure 4. Conceptual D-Strut Design Dimensions

FIVE-PARAMETER MODEL

Analytical models were developed for the stiffness, damping, and stress of each of the components shown in Figure 4. In the case of the tubes, the stiffnesses K_1 and K_2 are simply A_1E_1/L_1 and A_2E_2/L_2 for the respective members. For the diaphragm, however, the static stiffness (K_3) is a complicated function of the dimensions a, b, and h and the diaphragm modulus of elasticity, E_d. Damping (C) is calculated from the fluid viscosity, μ, and orifice dimensions, d and L. An additional stiffness (K_4) is calculated for the diaphragm/fluid cavity to account for the compressability of the fluid and the finite volumetric stiffness of the diaphragm. This stiffness involves parameters a, b, h, g, the diaphragm modulus of elasticity, E_d, and the fluid bulk modulus, K_f.

A complete dynamic model of this system is indicated in Figure 5. In this model, there are now five parameters: K_1 through K_4 and C. The mechanical impedance of the complete five-parameter model is:

$$Z5(s) = \frac{F}{X_1} = \frac{(K_1K_2+K_1K_3+K_2K_3)K_4 + (K_2K_4+K_1K_2+K_1K_3+K_1K_4+K_2K_3)Cs}{(K_2+K_3)K_4 + (K_2+K_3+K_4)Cs} \qquad (10)$$

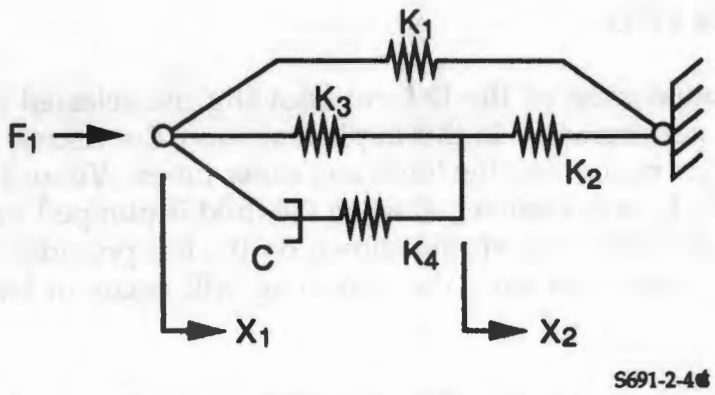

Figure 5. D-Strut Detailed Model

This transfer function is of the form:

$$Z5(s) = K_{EQ}(1+s/\omega_Z)/(1+s/\omega_P) \quad (11)$$

where,

$$\omega_Z = (K_1K_2+K_1K_3+K_2K_3)K_4/(K_2K_4+K_1K_2+K_1K_3+K_1K_4+K_2K_3)C \quad (12)$$

$$\omega_P = (K_2+K_3)K_4/(K_2+K_3+K_4)C \quad (13)$$

$$K_{EQ} = (K_1K_2+K_1K_3+K_2K_3)/(K_2+K_3) \quad (14)$$

EQUIVALENCE OF THREE- AND FIVE-PARAMETER MODELS

Typically, the stiffness due to fluid compressibility and damping chamber expansion, K_4, is large, and the stiffness due to diaphragm flexure, K_3, is small compared to K_1 and K_2. If $K_4 = \infty$ and $K_3 = 0$ are substituted into (10) through (14), these equations reduce to (1) through (3), with $K_A = K_1$, $K_B = K_2$ and $C = C_A$. However, it is also possible to establish an equivalence between the three-parameter and five-parameter mechanical impedance models with finite, non-zero values for K_3 and K_4.

Equating the static stiffnesses:

$$K_A = (K_1K_2+K_1K_3+K_2K_3)/(K_2+K_3) \quad (15)$$

Equating the zero and pole frequencies:

$$K_AK_B/(K_A+K_B)C_A = (K_1K_2+K_1K_3+K_2K_3)K_4/(K_2K_4+K_1K_2+K_1K_3+K_1K_4+K_2K_3)C \quad (16)$$

$$K_B/C_A = (K_2+K_3)K_4/(K_2+K_3+K_4)C \quad (17)$$

Equations (16) and (17) can be solved simultaneously for the two unknowns K_B and C_A:

$$K_B = K_2^2 K_4/[(K_2+K_3+K_4)(K_2+K_3)] \quad (18)$$

$$C_A = [K_2/(K_2+K_3)]^2 C \quad (19)$$

This equivalence is significant because it allows the three-parameter model to describe the D-Strut dynamics just as accurately as the five-parameter model.

D-STRUT PARAMETER SYNTHESIS

In the above section, it was shown that an equivalent three-parameter model could be used to represent the dynamics of a five-parameter D-Strut. In the detailed design of a D-Strut, however, it is necessary to utilize the five-parameter model, because it is these parameters that can be related to specific physical quantities (tube stiffnesses, diaphragm stiffnesses, etc). The relationship between the three-parameter and five-parameter models is not unique, and this fact may be used to develop a D-Strut optimized for minimum stress or weight without affecting its performance (i.e., its mechanical impedance).

To determine allowable values of the five-parameter D-Strut from the three-parameter description of the mechanical impedance, equations (15), (16), and (17) are solved with two additional constraint equations:

$$N = K_4/K_3 \quad (20)$$

$$M = K_2/K_1 \quad (21)$$

In addition to providing a closed solution, these two constraints make intuitive sense. M is the ratio if inner-to-outer-tube axial stiffness, and should generally be in the range $1 \le M \le 100$. N is the ratio of series-to-shunt stiffness of the diaphragm/fluid damper. Typically, one would expect N to also lie in the range $1 \le N \le 100$. As will be evident, the actual range of M and N to meet a specific mechanical impedance will be less.

The solution of the five equations noted above for the five unknowns is tedious, but there is a closed-form solution. In fact, there are two solutions, both of which are valid:

Letting

$$a = N(1+M) \quad (22)$$

$$b = K_A[\alpha^2(M-N)-(N+M+NM)] \quad (23)$$

$$c = \alpha^2 K_A^2 N \quad (24)$$

$$K_1 = [-b \pm (b^2 - 4ac)^{1/2}]/2a \quad (25)$$

$$K_2 = MK_1 \quad (26)$$

$$K_3 = [K_2(K_A-K_1)]/[K_2-(K_A-K_1)] \quad (27)$$

$$K_4 = NK_3 \quad (28)$$

$$C = NK_3(K_2+K_3)/\{\omega_2[K_2+K_3(1+N)]\} \quad (29)$$

For specific values of K_A, K_B, C_A, N, and M the above equations may produce complex or negative values for K_1, K_2, etc; however, where a positive real solution exists, two positive real solutions exist.

In order to minimize the D-Strut weight, M should be made as small as possible. There is, however, a minimum value of M once N is selected. Figure 6 illustrates this relationship for the PACOSS D-Strut case. Clearly, N should be made as high as possible, consistent with practical design and stress considerations. The point circled in Figure 6 shows the value for M and N ultimately selected for the PACOSS design.

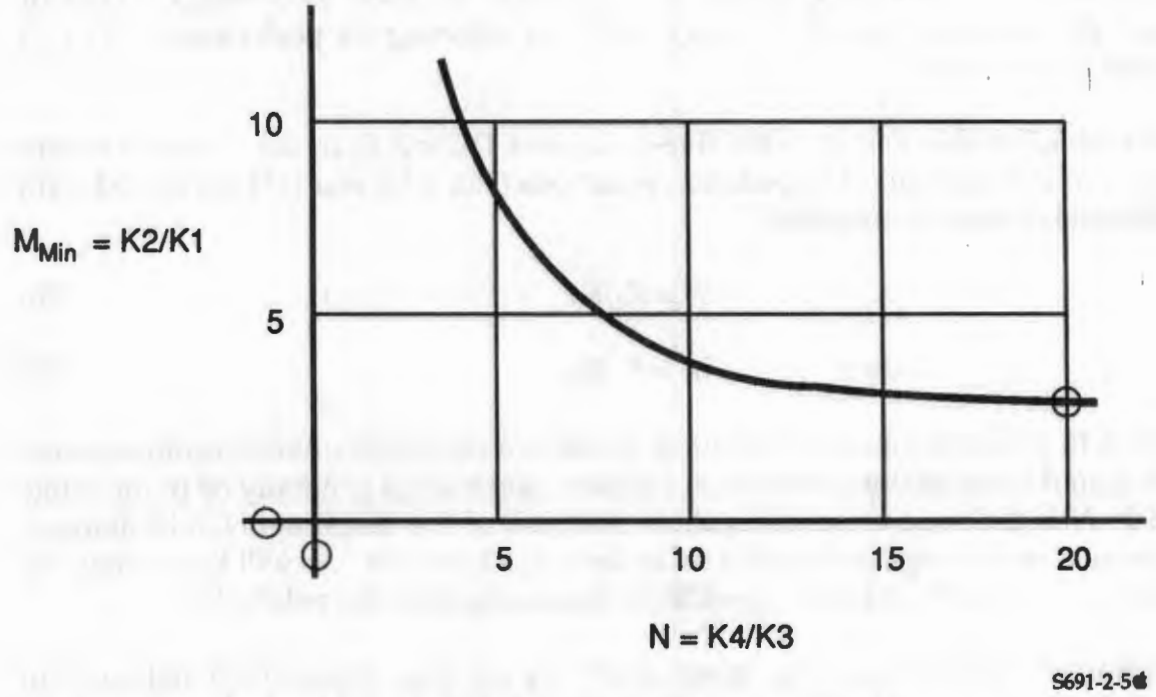

Figure 6. Minimum K2/K1 Versus K4/K3

D-STRUT FORCES

When sizing the D-Strut mechanical components, the applied forces are required in order to calculate static and dynamic loads, fluid pressures, stresses, etc. Let F_T denote the externally applied axial force. This force divides (dynamically) between the inner and outer tubes. Let F_I denote the force in the inner tube. Referring to Figure 5, $F_I = K_2X_2$; this leads to the following transfer function:

$$F_I/F_T(s) = K_2K_3(1+s/\omega_3)/[(K_2+K_3)K_A(1+s/\omega_1)] \quad (30)$$

where,

$$\omega_3 = K_3K_4/[(K_3+K_4)C] \quad (31)$$

The force in the inner tube depends not only on the ratio of stiffnesses, but on the frequency content of the applied force. Two cases are of interest:

(1) F_T is a sinusoid of magnitude F_T and frequency w_0. In this case the magnitude of F_I is obtained by substituting jw_0 for s in equation (30).

(2) F_T is a step function of magnitude F_T. The force in the inner tube is then an exponentially decayed step, which has an initial value F_D and a final value F_S (referred to as the dynamic and static forces, respectively). F_S is obtained by setting s to zero in (30), while F_D is obtained by letting s approach infinity.

$$F_S = F_TK_2K_3/[K_A(K_2+K_3)] \quad (32)$$

$$F_D = F_TK_2K_3\omega_1/[K_A(K_2+K_3)\omega_3] \quad (33)$$

DESIGN OPTIMIZATION PROCEDURE

The flow chart shown in Figure 7 summarizes the design procedure.

Steps 1 through 3 determine a set of the five parameter model values meeting the specified requirements. The selection of M and N is arbitrary, but if the limitation shown in Figure 6 is violated, the computed stiffnesses will be imaginary.

Steps 4 through 13 are used to size a diaphragm and damper meeting the required K_3, K_4, and C. This is done iteratively for various diaphragm aspect ratios (the ratio of diaphragm outside diameter to inside diameter, η), and the peak stresses and deflections are calculated under the two conditions of peak static and dynamic loads. An optimum design is then selected to provide the minimum peak stress and a peak diaphragm deflection less than the fluid gap.

To complete the design, Steps 15 through 17 are used to size the tubing thickness to provide the required K_1 and K_2. Each design corresponds to one row in Table 1. Steps 4 through 17 must be performed twice for each set of five parameter requirements determined in Steps 1 through 3 because there are two valid solutions for each assumed M and N. In Table 1, the two solutions are distinguished by the notation ' or – under the column "Sln."

In Step 18, the entire process (Steps 1 through 17) is repeated iteratively for alternative values of M and N. In Table 1, the best case (H) is underlined. Most of the cases run assumed the use of titanium for the diaphragm material. Beryllium copper was also evaluated, but found to produce a lower fatigue stress margin of safety.

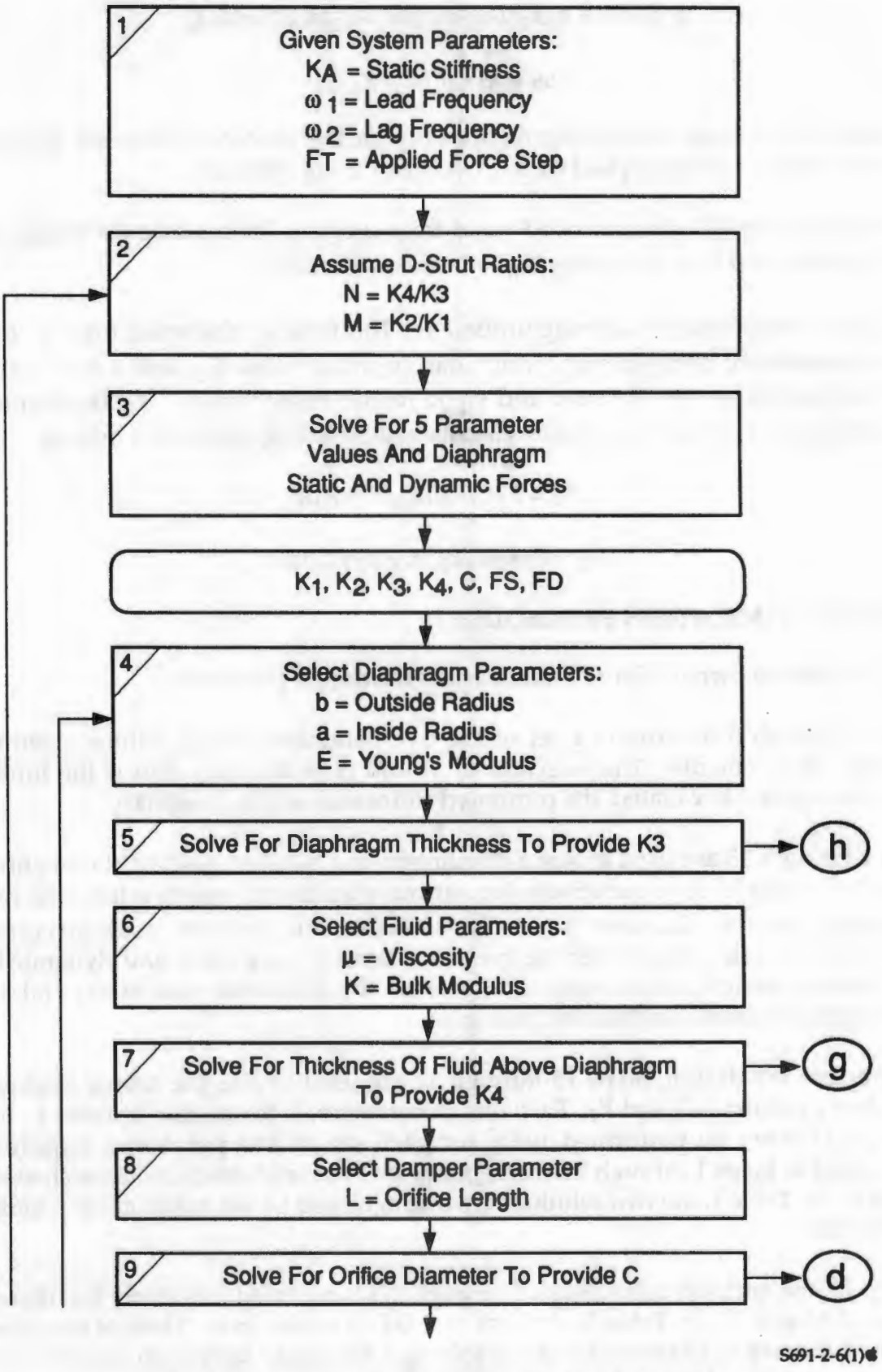

Figure 7. Design Optimization Procedure (Sheet 1)

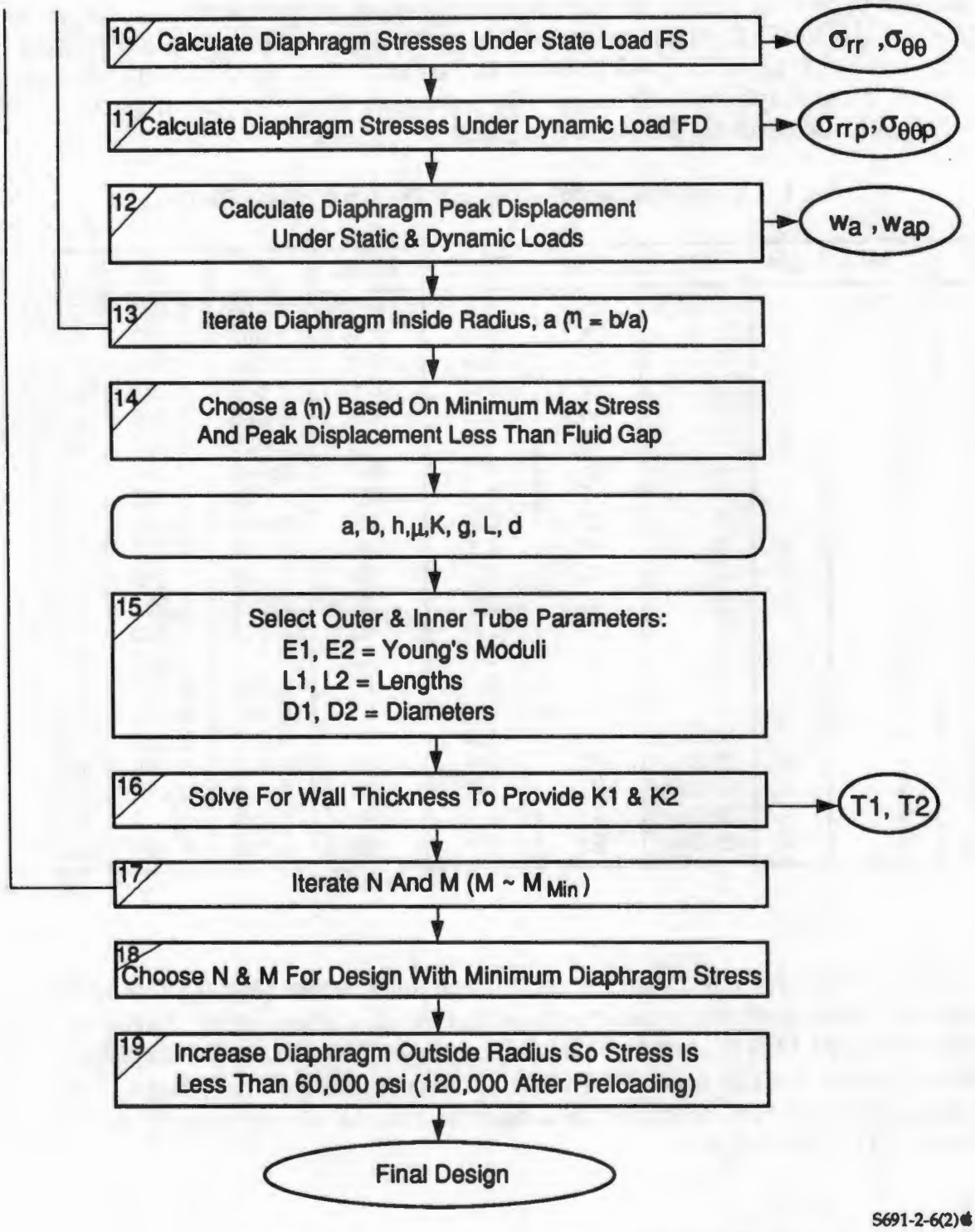

Figure 7. Design Optimization Procedure (Sheet 2)

The stresses shown in Table 1 do not include the effect of fluid preload. To prevent cavitation when the D-Strut is used in tension rather than compression, the preload is typically selected to equal the peak pressure in the fluid. This has the effect of doubling the stresses in the diaphragm. Therefore, the minimum stress design will be 2 x 77,000 = 154,000 psi, which exceeds the 120,000-psi limit for titanium.

Table 1. Optimum Diaphragms for 0.75-inch Outside Radius

N	M	Sln	Mtl	Case	OD/ID	Stress	h	g	wa
297	1.543	–	Ti	G	1.2	117	0.005	0.043	0.007
40	8	–	Ti	X	1.4	136	0.007	0.607	0.007
40	8	'	Ti	Y	1.6	116	0.030	0.010	0.005
40	4	–	Ti	V	1.4	116	0.008	0.471	0.007
40	4	'	Ti	W	1.6	112	0.026	0.016	0.005
20	32	–	Ti	R	1.4	112	0.009	0.851	0.007
20	32	'	Ti	S	2.0	100	0.046	0.010	0.004
20	8	–	Ti	T	1.4	101	0.009	0.720	0.007
20	8	'	Ti	U	2.0	99	0.041	0.014	0.005
20	4	–	Ti	P	1.6	86	0.014	0.357	0.007
20	4	'	Ti	Q	2.2	91	0.038	0.012	0.006
20	3	=	Ti	H	2.0	77	0.021	0.098	0.007
10	8	–	Ti	C	1.8	83	0.019	0.420	0.007
10	8	'	Ti	D	3.2	93	0.056	0.010	0.005
10	4	–	Ti	A	3.0	81	0.038	0.042	0.006
10	4	'	Ti	B	3.0	85	0.041	0.033	0.006
20	4	–	BeCu	P1	1.4	94	0.010	0.530	0.007
20	3	–	BeCu	F1	2.0	86	0.020	0.098	0.007
10	8	–	BeCu	C1	1.8	91	0.018	0.420	0.007
10	4	–	BeCu	A1	3.0	91	0.036	0.042	0.006
7	6	–	BeCu	E1	3.0	93	0.035	0.109	0.007

S691-2-7

All the cases shown in Table 1 assume a diaphragm outside diameter (OD) of 1.5 inches (because our initial goal was to design a D-Strut having approximately the same OD as the undamped PACOSS struts.) In Table 2, the results of increasing the diaphragm OD are shown. These cases all assume the same optimum ratios for M, N, and η. The final entry shown (Case H4) provides an adequate fatigue stress margin and has a diaphragm OD of 2.0 inches.

Figure 8 is a cross section of the final design, and Figure 9 is a photograph of the prototype.

Table 2. Optimum Diaphragms for N=20, M=3, Sln=-

b	Mtl	Case	OD/ID	Stress	h	g	wa	p
0.625	BeCu	F2	2	110	0.018	0.068	0.007	493
0.750	BeCu	F1	2	86	0.020	0.098	0.007	343
0.875	BeCu	F3	2	70	0.022	0.134	0.007	252
1.000	BeCu	F4	2	59	0.025	0.174	0.007	193
1.250	BeCu	F5	2	44	0.028	0.273	0.007	123
1.500	BeCu	F6	2	34	0.032	0.392	0.007	86
0.625	Ti	H2	2	98	0.019	0.068	0.007	493
0.750	Ti	H1	2	77	0.021	0.098	0.007	343
0.875	Ti	H3	2	63	0.024	0.134	0.007	252
1.000	Ti	H4	2	50	0.026	0.174	0.007	193

S691-2-8

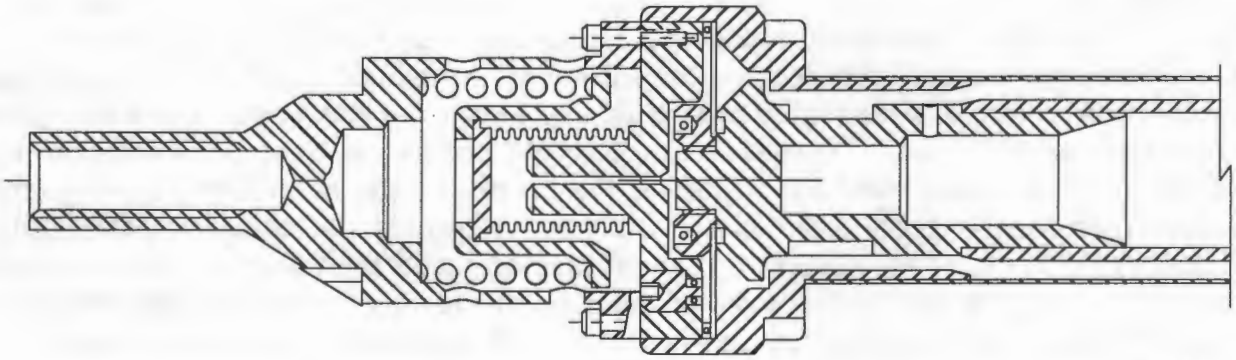

S691-2-9

Figure 8. Final Layout of PACOSS D-Strut

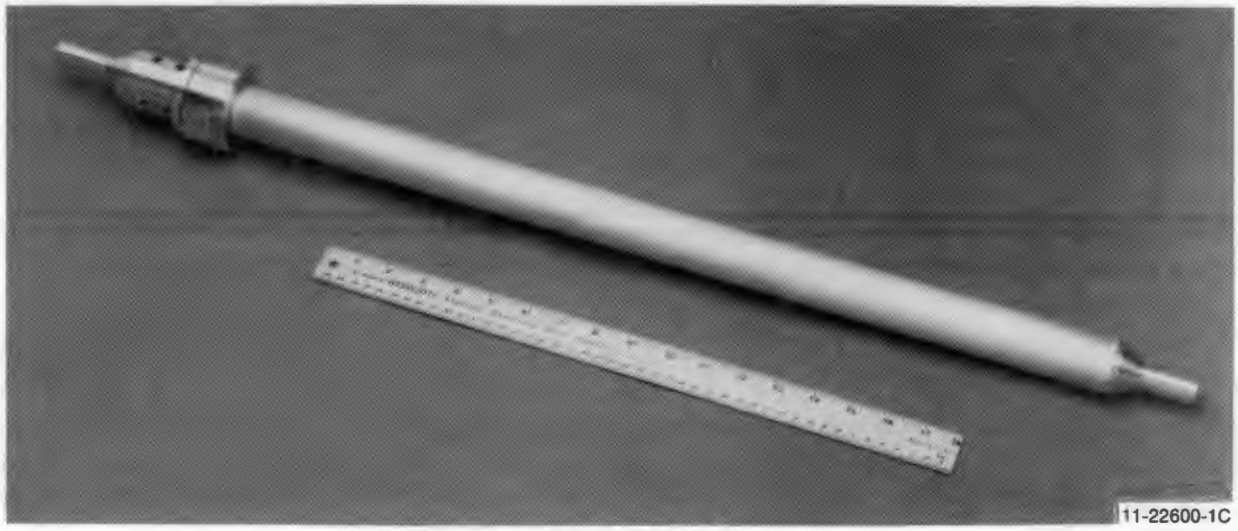

Figure 9. PACOSS D-Strut

D-STRUT CHARACTERIZATION

Testing of the D-Struts was conducted at CSA Engineering in Palo Alto, California, between January and April 1990. The mechanical impedance was measured using a shaker driving the D-Strut under test through a load cell with the other end of the D-Strut rigidly grounded. The differential displacement across the D-Strut was measured using a pair of Kaman eddy current proximeters. Calibration was verified with a "dummy" tube consisting of an outer tube (1.5-in. ODx.035-in. aluminum wall) mounted between two end fittings, which provided the same overall length and mechanical interface as the deliverable units. Both static and dynamic tests verified that the stiffness was equal to that calculated for the tube alone, and that the phase angle was only a few tenths of a degree.

In the succeeding tests, two basic procedures evolved. Static measurements were made by commanding the shaker with a 20-second period triangle waveform corresponding to ±500 lb force peak amplitude. The displacement was plotted by the Zonic analyzer against force so that the stiffness (slope), linearity, and hysteresis were readily apparent. Dynamic impedance was measured by applying a random noise having a flat Power Spectral Density (PSD) over a selected bandwidth. The input was controlled by a GenRad Servo Controller that monitored the force transducer output. Peak force and bandwidth can be independently controlled and a constant compressive or tensile force can be superimposed by the shaker amplifier electronics. A crest factor (peak-to-rms ratio) of 3.6 was assumed for adjusting the output of the controller. For dynamic impedance measurement, the Zonic analyzer computes the complex Fast Fourier Transfer (FFT) of the force and differential displacement, then displays the amplitude and phase angle of their ratio. Further details of the testing procedure are given in the paper, "Testing of a Viscous Damped Isolator," by B. Allen, also in these proceedings.

Figures 10 and 11 are plots of the magnitude and phase of the complex mechanical impedance of a typical D-Strut. Analysis of the test data indicates that the peak phase lead is about 16.5 degrees, which is less than the 22.6 degrees desired. Considerable effort was spent in an attempt to identify the source of the added compliance that caused this loss. The results of the development testing program showed that the added compliance was distributed between:

- Diaphragm edge clamping (both inner and outer edges)
- Low modulus in the inner tube aluminum
- Series compliance in the spring housing and end fittings
- Low shear modulus in the epoxy originally used

Alternative designs were also hypothesized, which would replace the diaphragm with (1) a piston, (2) an annular flexure, or (3) a bellows, which might provide a higher phase lead. Unfortunately, the schedule or funding did not permit our pursuing these approaches. These alternatives are discussed further in the paper "Design Trade Data on the Arch-Flexure D-Strut," by L. Porter Davis and Dr. Steve Ginter, also in these proceedings.

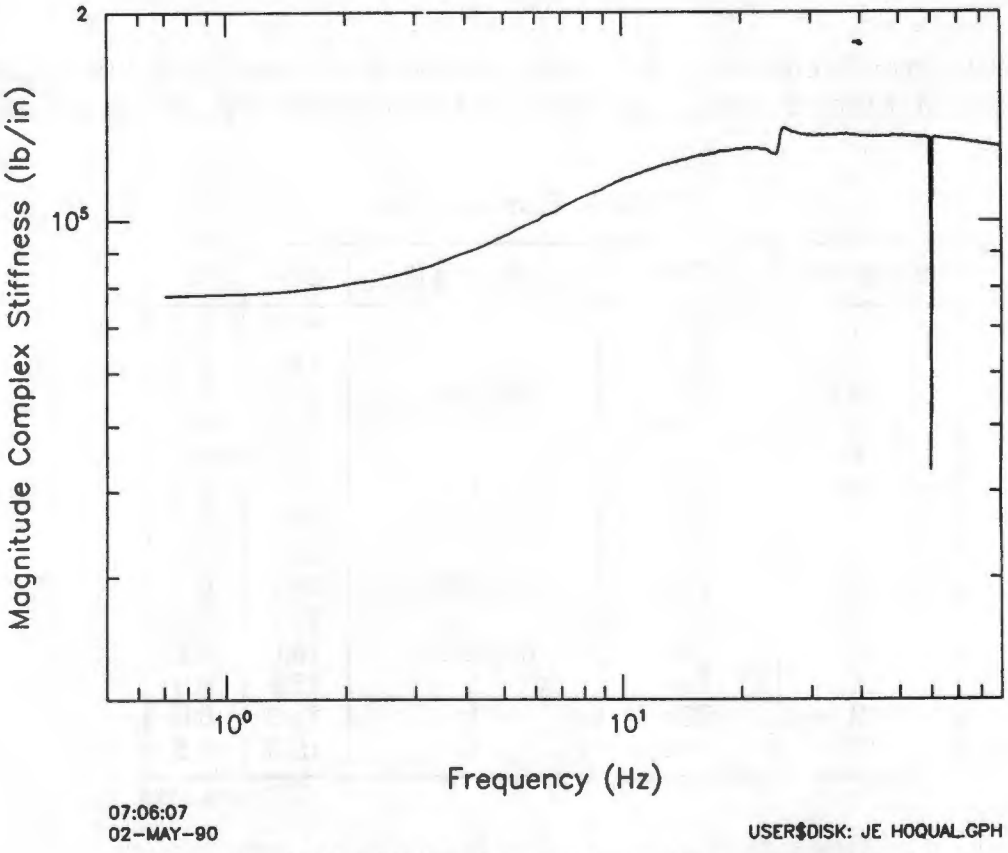

Figure 10. D-Strut 1 Mechanical Impedance – Magnitude

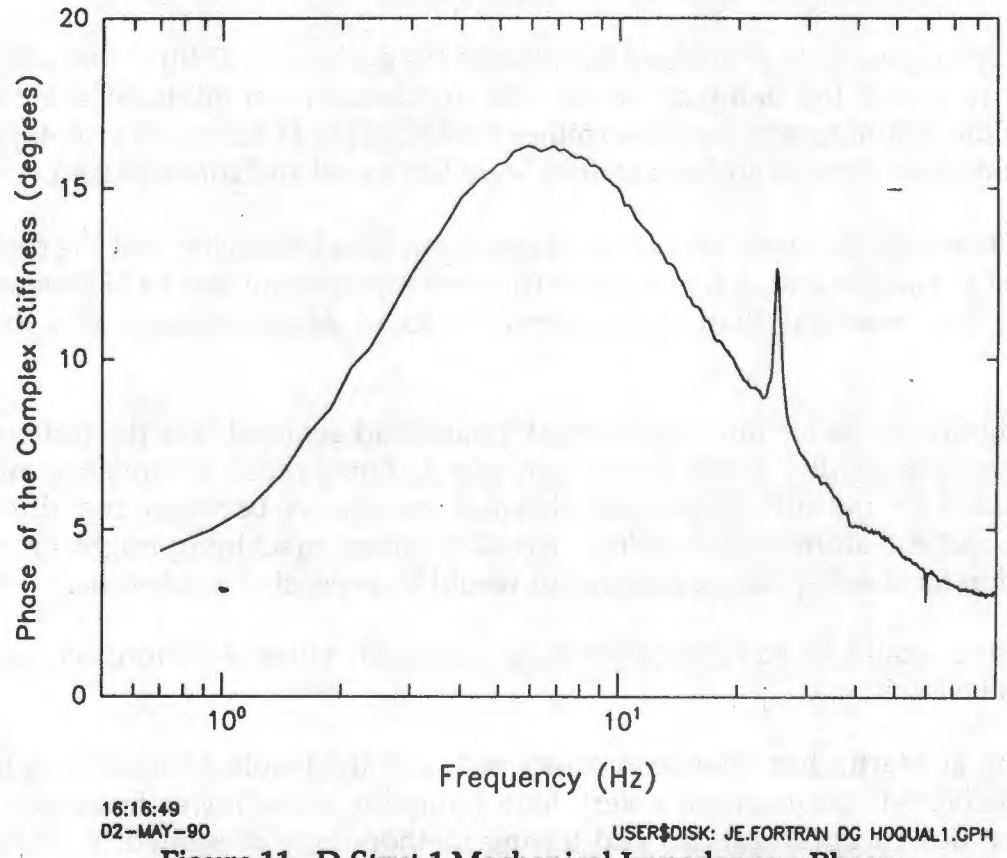

Figure 11. D-Strut 1 Mechanical Impedance – Phase

A total of 14 D-Struts were built, which incorporated improvements to the diaphragm edge clamping and tube bonding. Results of the characterization testing are listed in Table 3.

Table 3. Test Results

Serial No.	KSTATIC	Hysteresis (%)	ϕPK	f0
1	75k	1	16.5	6.5
2	71k	1	13.5	5.0
3	76k	negligible	14.5	5.0
4	74k	1	14.5	4.5
5	74k	1	15.5	6.0
6	69k	1	12.0	6.5
7	74k	1	13.0	6.5
8	71k	1	16.0	5.1
9	77k	negligible	16.7	6.5
10	73k	1	15.7	5.8
11	73k	negligible	16.0	6.2
12	72k	1	15.5	6.5
13	70k	1	15.0	6.0
14	72k	1	15.5	6.5

S691-2-136

CONCLUSIONS

Analytical techniques were developed to optimize the design of a D-Strut that utilized a diaphragm to pump the damping fluid. The optimization minimized the outside diameter of the diaphragm (which determines the OD of the D-Strut). A prototype unit was built and tested, and 14 additional units were fabricated and characterized.

The results were qualitatively very close to those predicted, showing that the dynamic models used to analyze and design the D-Strut were functionally correct. However, the peak phase lead was less than that desired (16 to 18 degrees versus 22.6 degrees desired).

The most significant factor limiting the peak phase lead achievable is the difficulty of obtaining bending rigidity of the diaphragm edges. Some radial compliance must be accommodated to permit differential thermal expansion between the titantium diaphragm and the aluminum housing. An all-titanium machining might provide a better solution for the diaphragm design, but would be expensive to fabricate.

An alternative would be to replace the diapragm with either a piston, an annular flexure, or a bellows.

Truss testing at Martin has now been completed, and the results indicate that the D-Struts, as delivered, demonstrate a very high damping of the lower frequency truss modes. The design optimizations and testing methodology presented in this paper should be of help in future D-Strut development.